


Linear and Nonlinear Dielectric Response of Intrinsically Disordered Proteins


Michael A. Sauer, Taylor Colburn, Sthitadhi Maiti, Matthias Heyden, and Dmitry V. Matyushov*


 Cite This: *J. Phys. Chem. Lett.* 2024, 15, 5420–5427

 Read Online

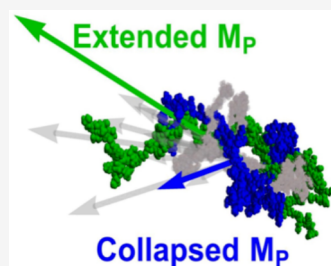
ACCESS |

 Metrics & More

 Article Recommendations

 Supporting Information

ABSTRACT: Linear and nonlinear dielectric responses of solutions of intrinsically disordered proteins (IDPs) were analyzed by combining molecular dynamics simulations with formal theories. A large increment of the linear dielectric function over that of the solvent is found and related to large dipole moments of IDPs. The nonlinear dielectric effect (NDE) of the IDP far exceeds that of the bulk electrolyte, offering a route to interrogate protein conformational and rotational statistics and dynamics. Conformational flexibility of the IDP makes the dipole moment statistics consistent with the gamma/log-normal distributions and contributes to the NDE through the dipole moment's non-Gaussian parameter. The intrinsic non-Gaussian parameter of the dipole moment combines with the protein osmotic compressibility in the nonlinear dielectric susceptibility when dipolar correlations are screened by the electrolyte. The NDE is dominated by dipolar correlations when electrolyte screening is reduced.



Proteins possess large dipole moments and can be detected by linear and nonlinear dielectric spectroscopies. Linear dielectric spectroscopy of protein solutions is a well-established field.^{1,2} The dielectric function of protein solutions allows one to determine two properties of the protein dipole vector \mathbf{M}_p : (1) the dipole mean-squared displacement $\langle \mathbf{M}_p^2 \rangle$ from the increment of the dielectric constant of the solution over that of the solvent and (2) the relaxation time of the dipole tumbling (β -peak in the dielectric spectrum).^{3,4} Dipole moments of many proteins from dielectric spectra have been reported⁵ based on Oncley's formulation.⁶ Employing dielectric spectroscopy to interrogate a protein's folding state through the alteration of $\langle \mathbf{M}_p^2 \rangle$ has been only marginally explored.⁷

The nonlinear dielectric response of protein solutions has not been reported to the best knowledge of these authors. Nonlinear spectroscopies in general allow measuring specific features not observable in linear spectroscopies, such as interfacial structure and dynamics.⁸ One therefore wonders if there are any advantages of using nonlinear dielectric techniques⁹ to interrogate proteins. The main difficulty of linear dielectric spectroscopy of proteins is a strong dielectric response of the electrolyte (ions and bulk water) requiring sufficiently large protein concentrations and the ensuing difficulties with protein aggregation.¹⁰ If a stronger contrast between proteins and electrolyte can be gained from nonlinear techniques, it would allow a more specific focus on the protein component.

The first exploration of this possibility¹¹ has indeed shown that the nonlinear dielectric effect (NDE) arising from proteins far exceeds that of the solvent. The NDE arises from correlations of protein dipoles if they are not screened by electrolyte. The inclusion of electrolyte screening in this study shows that it can strongly reduce the protein NDE thus

requiring more attention paid to relative protein and electrolyte concentrations. Nevertheless, we confirm a strong NDE arising from correlated dipoles of intrinsically disordered proteins^{12–14} (IDPs) studied here.

The NDE is quantified by the dielectric function of a solution $\epsilon_{\text{sol}}(E)$ being a function of the applied electric field E , in contrast to the linear dielectric constant of solution (a material property) ϵ_{sol} independent of the field. The difference $\epsilon_{\text{sol}}(E) - \epsilon_{\text{sol}}$ is linear in E^2 in the lowest order in E . The proportionality constant a is the Piekara coefficient:^{9,15–17} $\Delta\epsilon(E) = \epsilon_{\text{sol}}(E) - \epsilon_{\text{sol}} = aE^2$.

A nonzero value of a arises from non-Gaussian statistics of the z -projection M_z of the sample dipole moment,¹⁸ where the z -axis is chosen along the direction of the externally applied electric field. The Piekara coefficient in this notation becomes a product of the number of dipoles N in the sample and the term in the brackets in eq 1 quantifying the deviation of the statistics of M_z from a Gaussian distribution

$$a \propto N \left[1 - \frac{\langle M_z^4 \rangle}{3\langle M_z^2 \rangle^2} \right] \quad (1)$$

Here, an ensemble average $\langle \dots \rangle$ is taken over the sample configurations in the absence of the applied field, and $\langle M_z \rangle = 0$ is assumed. The term in the brackets in eq 1 vanishes for a

Received: March 22, 2024

Revised: May 7, 2024

Accepted: May 10, 2024

Published: May 14, 2024



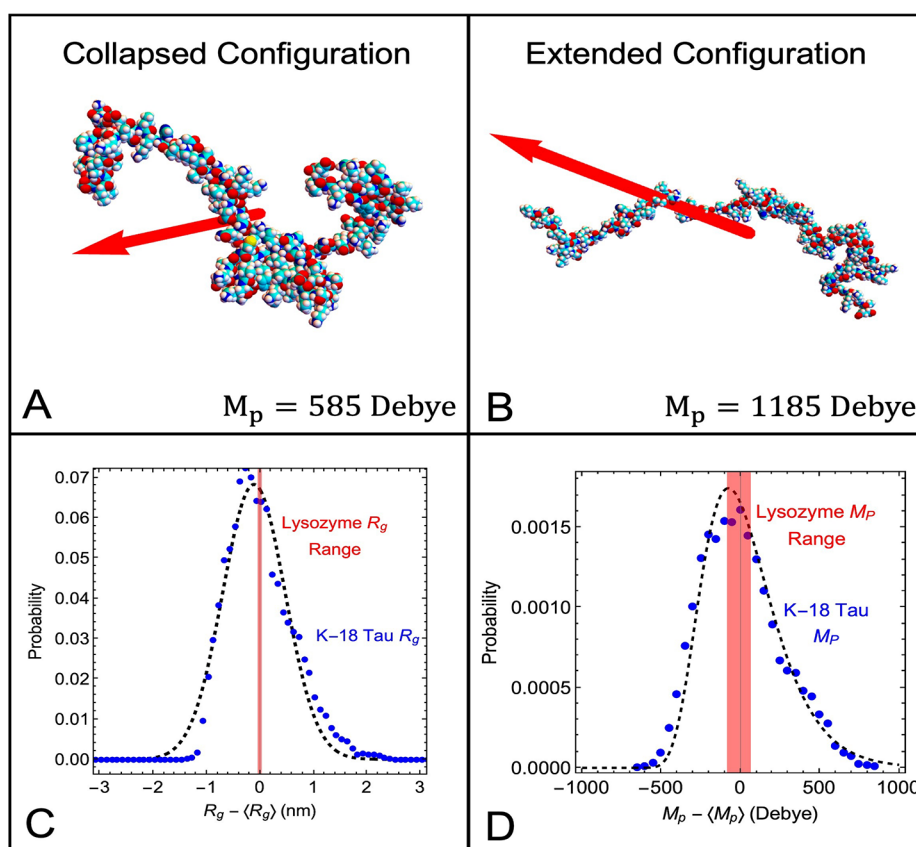


Figure 1. Collapsed (A) and extended (B) conformations of the Tau K-18 domain (simulated with A03ws) with the magnitude and direction of the dipole moment shown by red arrows. (C) The distribution of the radius of gyration R_g for A03ws is compared to the corresponding distribution for lysozyme. (D) The distribution of the dipole moment magnitude, $M_p = |M_p|$, for A03ws and lysozyme. The dashed lines are fits of MD data to Gaussian (C) and log-normal (D) distributions, and the widths of the red vertical lines correspond to the width of the corresponding distributions for lysozyme.

macroscopic sample with a large number of dipoles N as stipulated by the central limit theorem. This is avoided by multiplying the bracket term with N , thus producing a finite value. Consequently, the Piekara coefficient describes the first order, $\propto N^{-1}$, deviation of the statistics of the macroscopic dipole moment from the Gaussian limit. The dipole moment of the sample fluctuates due to conformational changes of individual proteins, their density fluctuations, and their rotations producing non-Gaussian statistics of M_z even in the limit of infinite dilution.¹⁹

The NDE was shown¹¹ to be highly sensitive to protein dipole interactions responsible for the scaling $a \propto M_p^8$ in the regime dominated by dipolar correlations. Because of this strong scaling, nonlinear dielectric spectroscopy can be used to monitor protein conformations and, potentially, physiological activity. IDPs or disordered domains of folded proteins²⁰ can be good candidates for observing NDE. Large fluctuations, by both rotations and conformational flexibility, of IDPs' dipole moments are also expected to produce a significant increment of the static dielectric constant of the protein solution ϵ_{sol} over that of the pure solvent, ϵ_s . The goal of this Letter is to quantify the linear and nonlinear dielectric response of IDPs. We combine molecular dynamics (MD) simulations of IDPs in force-field water with analytical theories delivering the corresponding experimental observables, the dielectric increment, and the Piekara coefficient, based on MD parameters.

All simulations²¹ were carried out with the GROMACS 2018.1 software package.²² A 130-residue (1986 atoms, 13.8

kDa) K-18 domain of the Tau protein was chosen for this study. The natural function of Tau proteins includes the stabilization of microtubules in the axons of neurons.²³ The K-18 domain of Tau protein is a subdomain of the overall Tau protein, consisting of four repeat microtubule binding regions.²⁴ Misfolding of Tau protein can lead to the formation of aggregates. The force fields (FFs) chosen here to describe K-18 are A03ws (AMBER03ws TIP4P/2005), A99*D (AMBER99SBws TIP4P/2005), and C36m* (CHARMM36m TIP3P), which incorporate modified protein–water interactions as described in ref 21; notations in the brackets specify the protein and water force fields. The FFs used here are nonpolarizable. Given that calculations of the dielectric response are based on the statistics of the dipole moment, direct screening of the external field by electronic polarization does not affect our calculations. According to general liquid-state theories,²⁵ molecular dipole moments get enhanced by electronic polarization, and this effect might be missing from the present simulations.

IDPs are highly disordered¹⁴ compared to folded proteins and produce large and highly fluctuating dipole moments (Figure 1A,B). The distributions of the radius of gyration²⁶ R_g follow the Gaussian statistics and are much broader than the corresponding distribution for folded lysozyme (Figure 1C). In contrast, the statistics of the protein dipole moment are very different from the Gaussian statistics that are applicable to lysozyme (Figure 1D) and require either log-normal or gamma distributions to fit the simulation data (see Figure S3 for

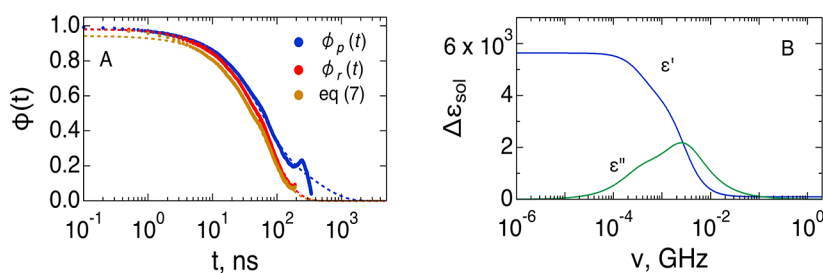


Figure 2. (A) Normalized correlation function of the protein dipole moment $\phi_p(t)$ and of the unit vector of the dipole moment orientation $\phi_r(t)$ (A03ws). The average correlation times are 160 ns ($\phi_p(t)$) and 69 ns ($\phi_r(t)$). Also shown is $\tilde{\phi}_p(t)$ (eq 7). The dashed lines refer to multiexponential fits. (B) Real (ϵ') and imaginary (ϵ'') parts of the increment dielectric function referring to proteins in solution calculated from eq 4 at $c_p = 0.1$ mM (1.4 mg/mL).

Table 1. Average $\langle R_g \rangle$, $\langle M_p \rangle$, and the Standard Deviation, σ_p ($\sigma_p^2 = \langle M_p^2 \rangle$), of the Protein Dipole (Debye)^a

FF	$\langle R_g \rangle^b$	$\langle M_p \rangle$	σ_p	χ_B	χ_r^c	τ_p	τ_r	$\Delta\epsilon_{\text{sol}}(0)^d$
A03ws	3.43	794	786	0.211	0.394	160	69	5637
A99*D	4.04	807	827	0.188	0.378	128	120	6242
C36m*	3.20	556	626	-0.355	0.402	141	35	3247

^aAlso listed are the non-Gaussian parameters χ_B and χ_r and the relaxation times of the protein dipole, τ_p , and of rotations of the dipole unit vector, τ_r (ns). ^bAverage radius of gyration (nm); standard deviations are listed in Table S1 and distributions are shown in Figure S1. ^cTheoretical value for the uniform distribution of orientations is $\chi_r = 0.4$. ^dCalculated at $c_p = 0.1$ mM (1.4 mg/mL).

comparison). This result suggests that extended conformations dominate in the distribution of the dipole moment²⁷ resulting in “fat tails” on the side of larger dipoles. While many IDPs follow Gaussian size distribution,²⁸ previous reports^{29–31} showed non-Gaussian size distributions resulting from conformational substates. Our results contrast between the Gaussian distribution of R_g and a strongly non-Gaussian distribution of M_p . The dipole moment of folded proteins scales, empirically, linearly with the protein size,³² suggesting similar statistics. Different statistics between these two parameters for IDPs do not allow for such a simple relation.

The NDE of IDPs has never been reported, and there are very few studies reported so far of the linear dielectric response of IDPs.^{33,34} We start by focusing on the linear dielectric response of IDP solutions, followed with the analysis of the NDE. The linear frequency-dependent dielectric function of the solution is given in terms of the time autocorrelation function of the solution dipole moment.^{35,36} The time scales of relaxation of the water and protein dipoles are widely separated, which allows us to look specifically at the time correlation function of the protein dipole. We therefore focus on the β -relaxation peak in the dielectric spectrum of the protein solution.¹ The corresponding normalized time correlation function of the protein dipole moment $\mathbf{M}_p(t)$ is

$$\phi_p(t) = \langle M_p^2 \rangle^{-1} \langle \mathbf{M}_p(t) \cdot \mathbf{M}_p(0) \rangle \quad (2)$$

where $\langle \mathbf{M}_p \rangle = 0$ is assumed as confirmed by simulations discussed below.

The time correlation function is next used in the standard linear-response formalism^{37–40} to calculate the frequency-dependent dielectric susceptibility. The connection between $\phi_p(t)$ and the dielectric increment, $\Delta\epsilon_{\text{sol}}(\omega) = \epsilon_{\text{sol}}(\omega) - \epsilon_s(\omega)$, of the solution ($\epsilon_{\text{sol}}(\omega)$) over the pure solvent ($\epsilon_s(\omega)$), neglects typically small^{38–40} cross correlations between protein and water dipole moments responsible for the δ -relaxation peak in dielectric spectra of protein solutions.⁴⁰

The frequency-dependent one-sided Fourier transform (Laplace–Fourier transform) $\tilde{\phi}_p(\omega)$ ($\omega = 2\pi\nu$) is obtained

from the fit of the time correlation function to a multiexponential function. The linear dielectric susceptibility function of a single protein molecule in the simulation box with the volume Ω follows from $\tilde{\phi}_p(\omega)$

$$\tilde{\chi}_p(\omega) = \frac{\langle M_p^2 \rangle}{3k_B T \Omega} (1 + i\omega\tilde{\phi}_p(\omega)) \quad (3)$$

To transform this result to conditions of dielectric experiments, one next considers the solution dielectric increment $\Delta\epsilon_{\text{sol}}(\omega)$ and assumes that the protein solution is sufficiently dilute to make protein dipoles statistically independent (the protein Kirkwood factor⁴¹ is equal to unity). The variance of the protein dipole moment is scaled with the number of noninteracting proteins N_p dissolved in the sample volume Ω . The resulting expression for the dielectric increment of solution becomes⁴⁰

$$\Delta\epsilon_{\text{sol}}(\omega) = c_p N_A [2\pi\beta \langle M_p^2 \rangle (1 + i\omega\tilde{\phi}_p(\omega)) - \Omega_p \Delta\epsilon_s(\omega)] \quad (4)$$

where $c_p = N_p / (N_A \Omega)$ is the molar concentration of proteins in the solution volume Ω , $\beta = (k_B T)^{-1}$ is the inverse temperature, N_A is the Avogadro number, and Gaussian units are used⁴² (in SI units, 2π would be replaced with $(2\epsilon_0)^{-1}$, where ϵ_0 is the vacuum permittivity). The second term in the brackets accounts for the reduction of the volume occupied by water when the solution is formed. Here, Ω_p is the average volume of a single protein and $\Delta\epsilon_s(\omega) = \epsilon_s(\omega) - \epsilon_\infty$, where ϵ_∞ is the high-frequency (electronic) limit of the dielectric function of the solvent (water). This term is dropped in our calculations, as it is typically small compared to the first term in eq 4.

The time correlation functions $\phi_p(t)$ from MD are shown in Figure 2A. Good fits of the correlation functions to multiexponential functions are achieved. The relaxation times listed in Table 1 are integrated times.

$$\tau_p = \int_0^\infty dt \phi_p(t) \quad (5)$$

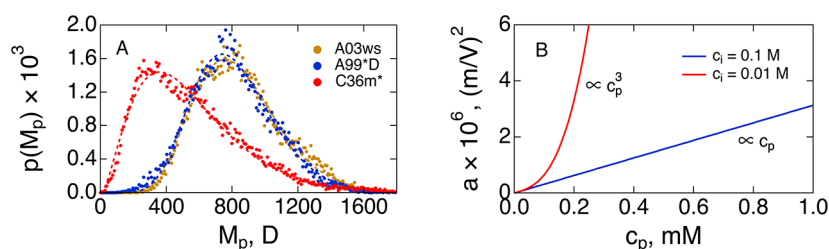


Figure 3. (A) Distributions of the magnitude of the protein dipole M_p for FFs listed in Table 1. The dashed lines, nearly indistinguishable on the plot scale for Amber FFs, refer to fits to gamma distributions with $\alpha = 11.2$ (A03ws), 10.5 (A99*D), and 2.8 (C36m*). (B) Piekara coefficient (eq 19) vs c_p at $c_i = 0.1$ and 0.01 M.

Laplace–Fourier transforms of the time correlation function are used in eq 4 to produce the increments of the dielectric function $\Delta\epsilon_{\text{sol}}(\omega)$ (of solution over water) shown in Figure 2B. The dielectric constant of the solution is significantly increased relative to the water solvent even at a submillimolar concentration of the protein ($\Delta\epsilon_{\text{sol}}(0) \simeq 5 \times 10^3$).

The dynamics of the dipole moment are driven by, potentially coupled, dipole rotations and conformational changes. To decouple these dynamics, one can look separately at the rotational correlation function of the directional unit vector of the protein dipole moment $\hat{\mathbf{e}}(t) = \mathbf{M}_p(t) / M_p(t)$

$$\phi_p(t) = \langle \hat{\mathbf{e}}(t) \cdot \hat{\mathbf{e}}(0) \rangle \quad (6)$$

This time correlation function is well-fitted to decaying exponents (Figure 2A). We have also explored if the dynamics of protein rotations can be decoupled from the dynamics of conformational changes. Given that $\mathbf{M}_p(t) = M_p(t)\hat{\mathbf{e}}(t)$, the assumption of dynamical decoupling leads to the following correlation function of the dipole moment

$$\bar{\phi}_p(t) = \langle M_p^2 \rangle^{-1} \langle M_p(t)M_p(0) \rangle \phi_p(t) \quad (7)$$

It is reasonably close to $\phi_p(t)$, except for a shorter tail, presumably cut off by faster rotations (Figure 2A). One can therefore view the IDP as a rotating dipole with conformational disorder sampled on time scales exceeding the rotational correlation time (Table 1).

To proceed to the nonlinear response, one can start with separating the statistics of protein rotations from statistics of conformations (the two components are also dynamically uncoupled, eq 7). Assuming an ideal solution (no interactions between the protein dipoles) and uncorrelated protein rotations, the distribution of polar angles θ projecting the dipole moment on the polar axis, $M_z = M\cos\theta$, becomes uniform. The statistical averages in eq 1 become

$$\langle M_z^n \rangle = \langle M_p^n \rangle_B \langle \cos^n \theta \rangle_\theta \quad (8)$$

where $\langle M_p^n \rangle_B$ is the n th statistical moment of the dipole moment in the body frame (subscript “B”). Assuming a uniform distribution $p(\theta) = 1/2$ for the polar angles θ , one obtains

$$\langle \cos^n \theta \rangle_\theta = \frac{1}{2m+1} \delta_{n,2m} \quad (9)$$

One can therefore calculate the non-Gaussian parameter characterizing conformational dynamics by rewriting eq 1 as

$$\chi_B = 1 - \frac{3\langle M_p^4 \rangle_B}{5\langle M_p^2 \rangle_B^2} \quad (10)$$

Fluctuations of the dipole moment in this frame are equivalent to fluctuations of the dipole moment magnitude M_p . The parameter χ_B is zero if M_p satisfies the Maxwell distribution. This is not the case for IDPs, and M_p follows the gamma distribution (Figure 3A)

$$P(x) \propto x^{\alpha-1} \exp[-x/\delta] \quad (11)$$

Equally good fits are obtained with the log-normal distribution $P(x) \propto \exp[-[\ln(x/x_0)]^2/(2\sigma^2)]$ (Figure S3). The average values of the dipole moment and the distributions of dipole moment magnitudes are distinctly different between AMBER and CHARMM FFs. These differences are consistent with histograms of the end-to-end distances, which closely reflect the differences between the corresponding dipole moment distributions (Figure S5).

The traditional theories of the NDE^{36,43} consider free rotations of dipoles in the liquid as the origin of the nonlinear dielectric response. In this case, the fluctuations of the dipole moment are neglected, and one arrives from eq 1 at the following expression for the rotational non-Gaussian parameter

$$\chi_r = 1 - \frac{\langle e_z^4 \rangle}{3\langle e_z^2 \rangle^2} \quad (12)$$

In the case of an isotropic distribution of angles θ , one obtains $\langle e_z^2 \rangle = 1/3$, $\langle e_z^4 \rangle = 1/5$, and $\chi_r = 2/5$. We indeed find χ_r calculated from MD to be close to this theoretical prediction (Table 1 and Figure S2), confirming the isotropic distribution of dipolar orientations and sufficient sampling of protein rotations.

The model of free dipolar rotations produces a nonzero and positive value of the non-Gaussian parameter in eq 1. This result contradicts the Langevin model of dipolar saturation, which always predicts a negative nonlinear dielectric response. The reason for the discrepancy is the silent assumptions made when the Langevin model for a single dipole in the external field is extended to an ensemble of dipoles. These assumptions include placing the dipoles to an incompressible solid and neglecting their orientational correlations. The first assumption is never satisfied for solutions, and the second requires electrolyte screening.

The result for the Piekara coefficient in the limit of dilute solutions of rigid dipoles⁴⁴ can be generalized to the problem of fluctuating dipoles. This solution is achieved by assuming statistical independence between rotations and conformational fluctuations of the protein dipole (see SI). Since nonlinear experiments are mostly done with oscillating external fields with the amplitude E_m ,⁹ one replaces E^2 with the $E_m^2/4$ in the equations for the NDE.⁴⁵ Assuming that the Piekara coefficient connects $\Delta\epsilon(E_m)$ to E_m^2 , one obtains

$$a = c_p \frac{\pi \beta^3 \langle M_p^2 \rangle^2 N_A}{4} \left[\frac{12}{5} \gamma (g_K - 1) + \frac{\chi_T}{\chi_T^{\text{id}}} - \chi_B \right] \quad (13)$$

In this equation, only the binary correlations between the protein dipoles in solution are included, and the higher-order correlations are dropped. Correspondingly, the Piekara coefficient includes the Kirkwood factor g_K quantifying binary orientational correlations between directional unit vectors \hat{e} and the isothermal osmotic compressibility^{37,46–48} χ_T scaled with the ideal-gas compressibility $\chi_T^{\text{id}} = (\rho_p k_B T)^{-1}$; $\rho_p = N_p / \Omega$ is the number density of proteins in solution. When $\chi_T = \chi_T^{\text{id}}$, the density fluctuations of proteins in solution follow the Poisson distribution of the ideal gas. If orientations of ideal-gas dipoles are uncorrelated ($g_K = 1$) and the compressibility is equal to the ideal-gas compressibility, the Piekara coefficient is positive. The non-Gaussian parameter $\chi_B = \chi_r = 2/5$ in eq 13 for rigid dipoles and the term in the bracket is equal to $3/5$. When, on the contrary, one assumes that independent dipoles are placed at sites of an incompressible lattice, then $\chi_T = 0$, and the Piekara coefficient becomes negative in accord with the Langevin model.^{36,43} The values $-0.4 < \chi_B < 2/5$ in Table 1 indicate that neither the model of rigid rotating dipoles nor the Gaussian model apply to IDP's dipole moment.

There is yet another parameter in eq 13 that reflects the statistics of conformational fluctuations of protein dipoles

$$\gamma = \frac{\langle M_p \rangle \langle M_p^3 \rangle}{\langle M_p^2 \rangle^2} \quad (14)$$

One gets $\gamma = 1$ for rigid rotating dipoles and $\gamma = 1 + (1 + \alpha)^{-1}$ for the dipole moment distributed according to the gamma distribution (eq 11). The latter result is close to the limit of rigid dipoles for $\alpha \simeq 10$ fitting the MD data for Amber FFs in Figure 3A. We, however, obtained $\alpha = 2.8$, $\gamma \simeq 1.3$ for the CHARMM FF.

The previous theoretical study of the NDE of protein solutions¹¹ has shown that the first summand in eq 13, arising from interactions between the protein dipoles, dominates for most practical conditions unless at very low protein concentrations. Electrolyte screening was not considered in that work, and here we add ionic screening to evaluate conditions allowing to extract χ_B from the Piekara coefficient. The goal is to learn about conformational statistics of the IDP from the NDE.

The starting point is the effective interaction potential for proteins in solution. The interaction between probe dipoles M_p at the distance $r = |\mathbf{r}_1 - \mathbf{r}_2|$ in a dielectric with the dielectric constant ϵ_s was analyzed by Høye and Stell⁴⁹ and can be written as follows

$$u(12) = -\epsilon_s \chi_c^2 M_p^2 e^{-\kappa r} \frac{D(12)}{r^3} \quad (15)$$

Here, κ is the Debye–Hückel screening length accounting for the electrolyte screening, and $D(12) = 3(\hat{\mathbf{e}}_1 \cdot \hat{\mathbf{r}})(\hat{\mathbf{r}} \cdot \hat{\mathbf{e}}_2) - (\hat{\mathbf{e}}_1 \cdot \hat{\mathbf{e}}_2)$ is a rotational invariant⁵⁰ based on unit vectors $\hat{\mathbf{e}}_{1,2}$ of two protein dipoles. Eq 15 thus describes the dipole–dipole interaction energy screened by electrolyte ions. The parameter χ_c in this equation is the cavity field susceptibility. It is equal to the ratio of the local field acting on the dipole and the field of the external charges.⁵¹ The cavity field depends on the boundary conditions applied to the solvent dipoles at the

dielectric cavity surface. The cavity field susceptibility can generally be written as⁵²

$$\chi_c = \chi_c^L - \alpha \frac{2(\epsilon_s - 1)^2}{3\epsilon_s(2\epsilon_s + 1)} \quad (16)$$

where $\chi_c^L = (2 + \epsilon_s)/(3\epsilon_s)$ is the Lorentz cavity field,⁴³ and the parameter $0 \leq \alpha \leq 1$ switches between the Lorentz cavity at $\alpha = 0$ and the Maxwell cavity, $3/(2\epsilon_s + 1)$, at $\alpha = 1$. The Høye–Stell derivation⁴⁹ leads to χ_c^L in eq 15, as supported by microscopic simulations.⁵¹ The cavity field susceptibility was empirically found to be $\chi_c \simeq 1.2$ – 1.4 for proteins.^{40,52}

Protein conformations producing the non-Gaussian statistics of the protein dipole moment contribute a small negative term to the NDE of the protein solution (χ_B in eq 13), which is subtracted from the osmotic compressibility term. Dipolar orientational correlations lead to $g_K > 1$ in eq 13. Perturbation theories^{53–56} for g_K can be used at sufficiently weak dipole–dipole interactions producing the following result (SI)

$$g_K - 1 = \frac{17}{16} y_p^2 e^{-2\kappa\sigma} \quad (17)$$

The effective diameter of the protein σ , arising from the repulsive protein cores in protein–protein interactions, enters the exponential electrolyte screening term in g_K . The dimensionless polarity parameter^{36,43} y_p for proteins in solution is given by the equation

$$y_p = c_p \frac{4\pi\beta N_A}{9} \epsilon_s \chi_c^2 \langle M_p^2 \rangle \propto c_p \langle M_p^2 \rangle \quad (18)$$

From eqs 17 and 18, one finds that g_K scales as $c_p^2 \langle M_p^2 \rangle^2$ with the protein concentration and its dipole moment.

To simplify the analysis, we rewrite eq 13 in a more practical form for solutions at $T = 300$ K. Assuming the ideal-gas compressibility at a sufficiently small protein concentration, $\chi_T^{\text{id}} = (\rho_p k_B T)^{-1}$, and adopting $\gamma \simeq 1$, one obtains

$$a \simeq 2.13 \times 10^{-18} c_p \Delta^2 \left[\frac{12}{5} (g_K - 1) + 1 - \chi_B \right] \quad (19)$$

Here, we have introduced the dielectric increment parameter^{1,57} $\Delta = \Delta\epsilon_{\text{sol}}/c_p$ often reported from linear dielectric spectroscopy of protein solutions.

The magnitude and the concentration dependence of the NDE are strongly affected by the electrolyte concentration. When dipolar correlations are screened, one obtains $g_K - 1 \ll 1$ and $a \propto c_p \langle M_p^2 \rangle^2$. A positive contribution from $g_K - 1$ becomes dominant with decreasing ionic strength, and the NDE gains a strong, $\propto c_p^3 \langle M_p^2 \rangle^4$, scaling with the protein concentration¹¹ (Figure 3B). This result is based on the perturbation expansion for g_K (eq 17). One anticipates that mutual screening between the dipoles will result in saturation of g_K at higher protein concentrations and the return of a linear scaling $\propto c_p$. Measurements of the crossover from $a \propto c_p^3$ to $a \propto c_p$ (Figure 3B) should help in establishing limits of applicability of perturbation theories to g_K and will potentially allow building quantitative models of dipolar correlations of highly polar solutes in solution. The effect of electrolyte is more complex as ionic screening also affects IDP's compaction^{28,30,31,58,59} thus altering $\langle M_p^2 \rangle$.

Assuming the conservative⁴⁹ Lorentz form $\chi_c \simeq 1/3$ for the cavity field susceptibility,⁴³ one obtains $y_p \simeq 12.9$ at $c_p = 0.1$ mM. Combined with this large number, a large dielectric increment $\Delta \simeq 6.7 \times 10^7 \text{ M}^{-1}$ (A03ws in Table 1) results in a

substantial NDE with $a \approx 3.3 \times 10^{-7}$ (m/V)² at room temperature and the physiological $c_i = 0.1$ M for the electrolyte concentration entering the Debye–Hückel screening parameter for water, $\kappa = \sqrt{c_i}/0.3$ nm⁻¹. The latter is combined in the screening exponent in eq 17 with the protein diameter $\sigma = 2\sqrt{5/3}\langle R_g \rangle$ obtained from the average radius of gyration in Table 1 assuming a spherical protein shape (this number falls between $R_g/R_h \approx 1.5$ for the θ solvent^{60,61} and $R_g/R_h \approx 0.8$ – 0.9 for a globule, $R_h \approx \sigma/2$ is the hydrodynamic radius). The resulting Piekara coefficient for protein solutions needs to be compared to the Piekara coefficient of bulk water⁶² $a = -0.8 \times 10^{-15}$ (m/V)², which is 8 orders of magnitude lower. Clearly, IDPs establish a high contrast to the nonlinear response of the surrounding electrolyte solution.

The NDE due to dipolar correlations is positive, while the standard assignment of the NDE to dipolar saturation in the Langevin model produces a negative NDE.⁴³ A negative contribution to a also comes from the non-Gaussian statistics of the dipole moment adding a term $-\chi_B$ in eq 13. The use of perturbation theories for g_K is conditioned on the assumption that the interaction between the dipoles is less than $k_B T$ at the average distance between them $\langle r \rangle$. Even though large dipoles of IDPs strongly increase the interaction, it is mostly screened by the electrolyte at ionic concentrations of $c_i \approx 0.1$ M for the large average separation of $\langle r \rangle \approx 32$ nm at $c_p = 0.1$ mM. Correspondingly, one gets $\beta u(\langle r \rangle) \approx 4.7$ (eq 15) without electrolyte screening and $\approx 10^{-14}$ when screening at $c_i = 0.1$ M is applied to IDPs in Table 1. The condition of weak interactions between the dipoles extends to the protein concentration of $c_p \sim 10$ mM at $c_i = 0.1$ M. The range of theory applicability is strongly affected by the electrolyte concentration.

In summary, we find that large and strongly fluctuating dipoles of IDPs in solution do not follow the Gaussian/Maxwell statistics and are instead reasonably fitted by the gamma/log-normal distributions. Large protein dipoles contribute significantly to the dielectric increment of the protein solution. A large dielectric increment for unfolded proteins offers both the possibility of monitoring the protein folding state and altering the dielectric constant of solution by protein folding/unfolding. Mechanical forces are produced by polarized solutions,⁶³ and induction of mechanical forces by protein denaturation, leading to a higher dielectric constant of the solution, is an intriguing possibility. Non-Gaussian statistics of the IDP's dipole moment makes a relatively small contribution to the solution NDE, which is dominated by correlations of protein dipoles and solution's osmotic compressibility. The solution NDE is strongly affected by electrolyte screening that controls the turnover between the cubic, $\propto c_p^3 M_p^8$, and linear, $\propto c_p M_p^4$, scalings of the NDE with the protein concentration. The non-Gaussian parameter χ_B (Table 1) shows a noticeable sensitivity to FFs used in simulations (also see Figures S1–S4). The NDE can thus be used for FF development. We find that dipole moment distributions and resulting nonlinear dielectric responses are highly sensitive reporters of specific aspects of protein conformational ensembles.

■ ASSOCIATED CONTENT

SI Supporting Information

The Supporting Information is available free of charge at <https://pubs.acs.org/doi/10.1021/acs.jpcllett.4c00866>.

Simulation protocol, derivation of equations, and the analysis of time correlation functions from MD simulations (PDF)

Transparent Peer Review report available (PDF)

■ AUTHOR INFORMATION

Corresponding Author

Dmitry V. Matyushov – School of Molecular Sciences and Department of Physics, Arizona State University, Tempe, Arizona 85287-1504, United States; orcid.org/0000-0002-9352-764X; Email: dmitrym@asu.edu

Authors

Michael A. Sauer – School of Molecular Sciences, Arizona State University, Tempe, Arizona 85287-1504, United States

Taylor Colburn – Department of Physics, Arizona State University, Tempe, Arizona 85287-1504, United States

Sthitadhi Maiti – School of Molecular Sciences, Arizona State University, Tempe, Arizona 85287-1504, United States

Matthias Heyden – School of Molecular Sciences, Arizona State University, Tempe, Arizona 85287-1504, United States; orcid.org/0000-0002-7956-5287

Complete contact information is available at:

<https://pubs.acs.org/doi/10.1021/acs.jpcllett.4c00866>

Notes

The authors declare no competing financial interest.

■ ACKNOWLEDGMENTS

This research was supported by the National Science Foundation (CHE-2154465 (DVM) and CHE-2154834 (MH)). The supercomputer time was provided through ASU's Research Computing.

■ REFERENCES

- (1) Grant, E. H.; Sheppard, R. J.; South, G. P. *Dielectric Behaviour of Biological Molecules in Solution*; Clarendon Press: Oxford, 1978.
- (2) Takashima, S. *Electrical Properties of Biopolymers and Membranes*; Taylor & Francis, 1989.
- (3) Pethig, R. Protein-water interactions determined by dielectric methods. *Annu. Rev. Phys. Chem.* **1992**, *43*, 177–205.
- (4) Oleinikova, A.; Sasisanker, P.; Weingärtner, H. What can really be learned from dielectric spectroscopy of protein solutions? A case study of Ribonuclease A. *J. Phys. Chem. B* **2004**, *108*, 8467.
- (5) Takashima, S. Electric dipole moment of globular proteins: measurement and calculation with NMR and X-ray databases. *J. Non-Cryst. Solids* **2002**, *305*, 303–310.
- (6) Oncley, J. L. The investigation of proteins by dielectric measurements. *Chem. Rev.* **1942**, *30*, 433–450.
- (7) Ajaj, Y.; Wehner, M.; Weingärtner, H. Myoglobin and apomyoglobin in their native, molten globule and acid-denatured states. A dielectric relaxation study. *Z. Phys. Chem.* **2009**, *223*, 1105–1118.
- (8) Shen, Y. R. *The Principles of Nonlinear Optics*; Wiley-Interscience: NJ, 2003.
- (9) Richert, R. Supercooled liquids and glasses by dielectric relaxation spectroscopy. *Adv. Chem. Phys.* **2014**, *156*, 101–195.
- (10) Cametti, C.; Marchetti, S.; Gambi, C. M. C.; Onori, G. Dielectric relaxation spectroscopy of lysozyme aqueous solutions: Analysis of the delta-dispersion and the contribution of the hydration water. *J. Phys. Chem. B* **2011**, *115*, 7144–7153.
- (11) Matyushov, D. V. Nonlinear dielectric response of dilute protein solutions. *RSC Adv.* **2023**, *13*, 31123–31127.

- (12) Oldfield, C. J.; Dunker, A. K. Intrinsically disordered proteins and intrinsically disordered protein regions. *Annu. Rev. Biochem.* **2014**, *83*, 553–584.
- (13) Jakob, U.; Kriwacki, R.; Uversky, V. N. Conditionally and transiently disordered proteins: Awakening cryptic disorder to regulate protein function. *Chem. Rev.* **2014**, *114*, 6779–6805.
- (14) Mukhopadhyay, S. The dynamism of intrinsically disordered proteins: Binding-induced folding, amyloid formation, and phase separation. *J. Phys. Chem. B* **2020**, *124*, 11541–11560.
- (15) Piekara, A. A theory of electric polarization, electro-optical Kerr effect and electric saturation in liquids and solutions. *Proc. R. Soc.* **1939**, *172*, 360–383.
- (16) Piekara, A.; Chelkowski, A. New experiments on dielectric saturation in polar liquids. *J. Chem. Phys.* **1956**, *25*, 794–795.
- (17) Chelkowski, A. *Dielectric Physics*; Elsevier Scientific Pub. Co.: Amsterdam, 1980.
- (18) Matyushov, D. V. Nonlinear dielectric response of polar liquids. *J. Chem. Phys.* **2015**, *142*, 244502.
- (19) Han, Y.; Alsayed, A. M.; Nobili, M.; Zhang, J.; Lubensky, T. C.; Yodh, A. G. Brownian motion of an ellipsoid. *Science* **2006**, *314*, 626–630.
- (20) Schuler, B.; Soranno, A.; Hofmann, H.; Nettels, D. Single-molecule FRET spectroscopy and the polymer physics of unfolded and intrinsically disordered proteins. *Annu. Rev. Biophys.* **2016**, *45*, 207–231.
- (21) Maiti, S.; Heyden, M. Model-dependent solvation of the K-18 domain of the intrinsically disordered protein tau. *J. Phys. Chem. B* **2023**, *127*, 7220–7230.
- (22) Abraham, M. J.; Murtola, T.; Schulz, R.; Páll, S.; Smith, J. C.; Hess, B.; Lindahl, E. performance molecular simulations through multi-level parallelism from laptops to supercomputers. *SoftwareX* **2015**, *1*, 19–25.
- (23) Cleveland, D. W.; Hwo, S. Y.; Kirschner, M. W. Purification of tau, a microtubule-associated protein that induces assembly of microtubules from purified tubulin. *J. Mol. Biol.* **1977**, *116*, 207–225.
- (24) Yu, X.; Luo, Y.; Dinkel, P.; Zheng, J.; Wei, G.; Margittai, M.; Nussinov, R.; Ma, B. Cross-seeding and conformational selection between three- and four-repeat human Tau proteins. *J. Biol. Chem.* **2012**, *287*, 14950–14959.
- (25) Stell, G.; Patey, G. N.; Høye, J. S. Dielectric constants of fluid models: Statistical mechanical theory and its quantitative implementation. *Adv. Chem. Phys.* **1981**, *48*, 183–328.
- (26) Jephthah, S.; Staby, L.; Kragelund, B. B.; Skepö, M. Temperature dependence of intrinsically disordered proteins in simulations: What are we missing? *J. Chem. Theory Comput.* **2019**, *15*, 2672–2683.
- (27) Oltmann, H.; Reimann, J.; Will, S. Single-shot measurement of soot aggregate sizes by wide-angle light scattering (WALS). *Appl. Phys. B: Laser Opt.* **2012**, *106*, 171–183.
- (28) Müller-Späh, S.; Soranno, A.; Hirschfeld, V.; Hofmann, H.; Rügger, S.; Reymond, L.; Nettels, D.; Schuler, B. Charge interactions can dominate the dimensions of intrinsically disordered proteins. *Proc. Natl. Acad. Sci. U.S.A.* **2010**, *107*, 14609–14614.
- (29) Huang, F.; Rajagopalan, S.; Settanni, G.; Marsh, R. J.; Armoogum, D. A.; Nicolaou, N.; Bain, A. J.; Lerner, E.; Haas, E.; Ying, L.; et al. Multiple conformations of full-length p53 detected with single-molecule fluorescence resonance energy transfer. *Proc. Natl. Acad. Sci. U.S.A.* **2009**, *106*, 20758–20763.
- (30) Liu, W.-T.; Shen, Y. R. In situ sum-frequency vibrational spectroscopy of electrochemical interfaces with surface plasmon resonance. *Proc. Natl. Acad. Sci. U. S. A.* **2014**, *111*, 1293–1297.
- (31) Seth, S.; Stine, B.; Bhattacharya, A. Fine structures of intrinsically disordered proteins. *J. Chem. Phys.* **2024**, *160*, 014902.
- (32) Barlow, D. J.; Thornton, J. M. Charge distribution in proteins. *Biopolymers* **1986**, *25*, 1717–1733.
- (33) Reid, K. M.; Singh, A. K.; Bikash, C. R.; Wei, J.; Tal-Gan, Y.; Vinh, N. Q.; Leitner, D. M. The origin and impact of bound water around intrinsically disordered proteins. *Biophys. J.* **2022**, *121*, 540–551.
- (34) Reid, K. M.; Poudel, H.; Leitner, D. M. Dynamics of hydrogen bonds between water and intrinsically disordered and structured regions of proteins. *J. Phys. Chem. B* **2023**, *127*, 7839–7847.
- (35) Böttcher, C. J. F. *Theory of Electric Polarization. Dielectrics in Time-Dependent Fields*; Elsevier, 1973; Vol. 2.
- (36) Scaife, B. K. P. *Principles of Dielectrics*; Clarendon Press: Oxford, 1998.
- (37) Hansen, J.-P.; McDonald, I. R. *Theory of Simple Liquids*, 4th ed.; Academic Press: Amsterdam, 2013.
- (38) Boresch, S.; Höchtel, P.; Steinhauser, O. Studying the dielectric properties of a protein solution by computer simulation. *J. Phys. Chem. B* **2000**, *104*, 8743.
- (39) Boresch, S.; Willensdorfer, M.; Steinhauser, O. A molecular dynamics study of the dielectric properties of aqueous solutions of alanine and alanine dipeptide. *J. Chem. Phys.* **2004**, *120*, 3333.
- (40) Heyden, M.; Matyushov, D. V. Dielectrophoresis of proteins in solution. *J. Phys. Chem. B* **2020**, *124*, 11634–11647.
- (41) Fröhlich, H. *Theory of Dielectrics*; Oxford University Press: Oxford, 1958.
- (42) Jackson, J. D. *Classical Electrodynamics*, 2nd ed.; Wiley: New York, 1975.
- (43) Böttcher, C. J. F. *Theory of Electric Polarization: Dielectrics in Static Fields*, 2nd ed.; Elsevier: Amsterdam, 1973; Vol. 1.
- (44) Matyushov, D. V. Multiparticle orientational correlations are responsible for the nonlinear dielectric effect: Analysis of temperature-dependent measurements for glycerol. *J. Chem. Phys.* **2022**, *157*, 164501.
- (45) Richert, R.; Matyushov, D. V. Quantifying dielectric permittivities in the nonlinear regime. *J. Phys.: Condens. Matter* **2021**, *33*, 385101.
- (46) Chen, S.-H.; Bendedouch, D. Structure and interactions of proteins in solution studied by small-angle neutron scattering. *Methods Enzymol.* **1986**, *130*, 79–116.
- (47) Velev, O. D.; Kaler, E. W.; Lenhoff, A. M. Protein Interactions in Solution Characterized by Light and Neutron Scattering: Comparison of Lysozyme and Chymotrypsinogen. *Biophys. J.* **1998**, *75*, 2682–2697.
- (48) Gunton, J. D.; Shiryayev, A.; Pagan, D. L. *Protein Condensation*; Cambridge University Press: Cambridge, UK, 2007.
- (49) Høye, J. S.; Stell, G. Statistical mechanics of polar systems: Dielectric constant for dipolar fluids. *J. Chem. Phys.* **1974**, *61*, 562–572.
- (50) Gray, C. G.; Gubbins, K. E. *Theory of Molecular Liquids*; Clarendon Press: Oxford, 1984; Vol. 1: Fundamentals.
- (51) Martin, D. R.; Friesen, A. D.; Matyushov, D. V. Electric field inside a “Rosky cavity” in uniformly polarized water. *J. Chem. Phys.* **2011**, *135*, 084514.
- (52) Matyushov, D. V. Dipolar response of hydrated proteins. *J. Chem. Phys.* **2012**, *136*, 085102.
- (53) Rushbrooke, G. On the dielectric constant of dipolar hard spheres. *Mol. Phys.* **1979**, *37*, 761–778.
- (54) Tani, A.; Henderson, D.; Barker, J. A.; Hecht, C. E. Perturbation. *Mol. Phys.* **1983**, *48*, 863.
- (55) Goldman, S. Determination of static dielectric constant-temperature-density surfaces of a Stockmayer fluid by perturbation theory. *Mol. Phys.* **1990**, *71*, 491–507.
- (56) Gray, C. G.; Gubbins, K. E.; Joslin, C. G. *Theory of Molecular Liquids*; Oxford University Press: Oxford, 2011; Vol. 2: Applications.
- (57) South, G. P.; Grant, E. H. Dielectric dispersion and dipole moment of myoglobin in water. *Proc. R. Soc. London A* **1972**, *328*, 371–387.
- (58) Huihui, J.; Firman, T.; Ghosh, K. Modulating charge patterning and ionic strength as a strategy to induce conformational changes in intrinsically disordered proteins. *J. Chem. Phys.* **2018**, *149*, 085101.
- (59) Bianchi, G.; Longhi, S.; Grandori, R.; Brocca, S. Relevance of electrostatic charges in compactness, aggregation, and phase separation of intrinsically disordered proteins. *Int. J. Mol. Sci.* **2020**, *21*, 6208.

(60) Doi, M.; Edwards, S. F. *The Theory of polymer Dynamics*; Oxford University Press: Oxford, UK, 1986.

(61) Dünweg, B.; Reith, D.; Steinhauser, M.; Kremer, K. Corrections to scaling in the hydrodynamic properties of dilute polymer solutions. *J. Chem. Phys.* **2002**, *117*, 914–924.

(62) Davies, A. E.; van der Sluijs, M. J.; Jones, G. P.; Davies, M. Further study of high field dielectric effects in H₂O, D₂O and ionic solutions. *J. Chem. Soc., Faraday Trans. 2* **1978**, *74*, 571–578.

(63) Stratton, J. A. *Electromagnetic Theory*; McGraw-Hill Inc.: New York, 1941.